nature neuroscience

A long noncoding RNA contributes to neuropathic pain by silencing Kcna2 in primary afferent neurons

Xiuli Zhao[1,8], Zongxiang Tang[2,8], Hongkang Zhang[3,8], Fidelis E Atianjoh[1,8], Jian-Yuan Zhao[1,8], Lingli Liang[1], Wei Wang[1], Xiaowei Guan[1], Sheng-Chin Kao[1], Vinod Tiwari[1], Yong-Jing Gao[4], Paul N Hoffman[5], Hengmi Cui[6], Min Li[3], Xinzhong Dong[3,7] & Yuan-Xiang Tao[1]

Neuropathic pain is a refractory disease characterized by maladaptive changes in gene transcription and translation in the sensory pathway. Long noncoding RNAs (lncRNAs) are emerging as new players in gene regulation, but how lncRNAs operate in the development of neuropathic pain is unclear. Here we identify a conserved lncRNA, named Kcna2 antisense RNA, for a voltage-dependent potassium channel mRNA, *Kcna2*, in first-order sensory neurons of rat dorsal root ganglion (DRG). Peripheral nerve injury increased Kcna2 antisense RNA expression in injured DRG through activation of myeloid zinc finger protein 1, a transcription factor that binds to the *Kcna2* antisense RNA gene promoter. Mimicking this increase downregulated Kcna2, reduced total voltage-gated potassium current, increased excitability in DRG neurons and produced neuropathic pain symptoms. Blocking this increase reversed nerve injury–induced downregulation of DRG Kcna2 and attenuated development and maintenance of neuropathic pain. These findings suggest endogenous Kcna2 antisense RNA as a therapeutic target for the treatment of neuropathic pain.

Neuropathic pain is a major public health problem. Treatment for this disorder has had limited success owing to our incomplete understanding of the mechanisms that underlie the induction of neuropathic pain[1]. Nerve injury–induced neuropathic pain is thought to be triggered by abnormal spontaneous activity that arises in neuromas and first-order sensory neurons of the DRG[2,3]. The abnormal excitability may result from maladaptive changes in gene transcription and translation of receptors, enzymes and voltage-dependent ion channels in the DRG[4]. Voltage-dependent potassium channels govern cell excitability. Peripheral nerve injury downregulates expression of mRNA and protein for these channels in the DRG[5–10], a phenomenon that may contribute to induction of neuropathic pain[11–14]. However, the molecular mechanisms that underlie this downregulation are still unknown.

Recent studies suggest that the mechanism for gene regulation involves widespread noncoding RNAs, including lncRNAs[15–17]. The study of lncRNAs is still in its infancy[18,19]. A few lncRNAs have been identified in mammalian cells and implicated in gene-regulatory roles such as transcription and translation[18,19]. Their expression is associated with some physiological and pathological processes, but how they are causally linked to disease development is elusive[18,19]. Here, we report a new native lncRNA that is expressed in mammalian DRG neurons. Because most of its sequence is complementary to Kcna2 RNA, we named it Kcna2 antisense RNA. We found that Kcna2 antisense RNA may act as a biologically active regulator and participate in induction and maintenance of neuropathic pain by specifically silencing Kcna2 expression in the DRG.

RESULTS

Identification of natural Kcna2 antisense RNA in DRG neurons

To detect Kcna2 antisense RNA, we first searched a database using the complete published *Kcna2* cDNA sequence. Although many of the expressed sequence tags reflected portions of *Kcna2* transcript, a few were in the antisense direction. Using strand-specific primers for reverse transcription, we identified Kcna2 antisense transcript in the DRGs of rat, mouse, monkey and human (**Fig. 1a**), although the sequences were not identical among species. We also detected this transcript in spinal cord, various brain regions and other body organs of rats (**Supplementary Fig. 1a**). Using rapid amplification of cDNA ends for directional sequencing of 5′ and 3′ ends, we identified a 2.52-kb Kcna2 antisense RNA in rat DRG (**Supplementary Fig. 1b**). Most of its sequence overlapped that of *Kcna2* RNA, including the coding sequence, the 3′ untranslated region and part of the 5′ untranslated region, but Kcna2 antisense RNA had unique regions at the 5′ and 3′ ends (**Fig. 1b**). It had no apparent open reading frame (**Supplementary Fig. 1b**), indicating that Kcna2 antisense RNA is noncoding RNA.

We further confirmed the Kcna2 antisense RNA at the expected size by northern blot analysis of RNA from adult rat DRG and spinal cord,

[1]Department of Anesthesiology and Critical Care Medicine, Johns Hopkins University School of Medicine, Baltimore, Maryland, USA. [2]College of Basic Medicine, Nanjing University of Chinese Medicine, Nanjing, China. [3]The Solomon H. Snyder Department of Neuroscience, Johns Hopkins University School of Medicine, Baltimore, Maryland, USA. [4]Institute of Nautical Medicine, Jiangsu Key Laboratory of Neuroregeneration, Nantong University, Nantong, China. [5]Department of Ophthalmology, Johns Hopkins University School of Medicine, Baltimore, Maryland, USA. [6]Biomedical Innovation Institute, Yangzhou University, Yangzhou, China. [7]Howard Hughes Medical Institute, Johns Hopkins University School of Medicine, Baltimore, Maryland, USA. [8]These authors contributed equally to this work. Correspondence should be addressed to Y.-X.T. (ytao1@jhmi.edu).

Received 21 March; accepted 16 May; published online 23 June 2013; doi:10.1038/nn.3438

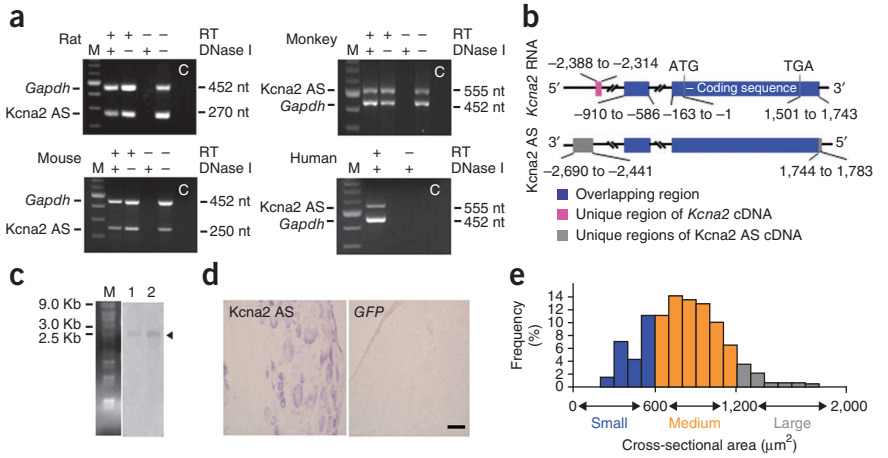

Figure 1 Identification and expression of Kcna2 antisense RNA in naive dorsal root ganglion. (**a**) Native Kcna2 antisense (AS) transcripts detected in the DRGs of rat (Sprague-Dawley), mouse (C57/BL6), monkey (*Macaca fascicularis*) and human using reverse transcription (RT)-PCR with strand-specific primers. To exclude genomic DNA contamination, we pretreated the extracted RNA samples with excess DNase I. *Gapdh* is a control. Without RT primers, neither *Gapdh* nor Kcna2 AS PCR products were detected in DNase I–treated samples, indicating absence of genomic DNA. $n = 3$ repeated experiments per species. We further confirmed the existence of native Kcna2 AS RNA in the tissues using specific intron-spanning primers. M, 100-bp ladder; C, no-template control. (**b**) The extent of sequence overlap (blue boxes) between the cDNAs of *Kcna2* RNA and Kcna2 AS RNA. (**c**) Northern blot expression analysis of Kcna2 AS RNA (arrowhead) in the DRG (lane 1) and spinal cord (lane 2) of rats. $n = 3$ repeated experiments. M, RNA marker. (**d**) *In situ* hybridization histochemistry showing the distribution of Kcna2 AS RNA in rat DRG. *GFP*, which is not expressed in mammalian cells, was used as a negative control. $n = 5$ rats. Scale bar, 40 μm. (**e**) Histogram shows the distribution of Kcna2 AS RNA–positive somata in normal rat DRG.

although the signals were weak (**Fig. 1c**). *In situ* hybridization histochemistry showed that Kcna2 antisense RNA was expressed weakly in DRG neurons (**Fig. 1d**). Approximately 21.5% of DRG neurons (228 of 1,060) were labeled. Most were medium-sized (69%; 25–35 μm in diameter), although some were small (24%; <25 μm in diameter) and a few large (7%; >35 μm in diameter) (**Fig. 1e**). Approximately 60.6% of Kcna2 antisense RNA–positive neurons were positive for neurofilament-200 (NF-200) protein, 18.1% for P2X3, 15.3% for isolectin B4 and 28.7% for calcitonin gene-related peptide (CGRP) (**Fig. 2**). Although the distribution pattern of Kcna2 antisense RNA partially overlapped that of Kcna2 protein in DRG (**Figs. 1e** and **3a**,**b**), most Kcna2 antisense RNA–positive neurons express low amounts of Kcna2 protein (**Fig. 3c**).

DRG Kcna2 antisense RNA expression after nerve injury

Next, we examined whether expression of DRG Kcna2 antisense RNA is altered in rat after peripheral nerve injury. Consistent with previous studies[5–10], unilateral fifth lumbar (L5) spinal nerve ligation (SNL), but not sham surgery, time-dependently downregulated *Kcna2* mRNA (**Fig. 4a**) and protein (**Fig. 4b**) in the ipsilateral L5 DRG. Notably, Kcna2 antisense RNA increased time-dependently in the ipsilateral L5 DRG after SNL (**Fig. 4c**). Neither SNL nor sham surgery changed the expression of *Kcna2* mRNA, Kcna2 protein or Kcna2 antisense RNA in the ipsilateral L4 DRG (**Fig. 4a**,**c**) or L5 spinal cord ($n = 4$ rats per group per time point, $P > 0.05$; **Supplementary Fig. 2a–c**). Furthermore, the staining density and number of Kcna2 antisense RNA–positive neurons in the ipsilateral L5 DRG were higher than those in the contralateral L5 DRG on days 3, 7 and 14 after SNL (**Fig. 4d**,**e**). These changes occurred predominantly in large DRG neurons (**Figs. 1e** and **4f**). Results were similar after sciatic nerve axotomy. On day 7 after axotomy, the ratio of ipsilateral to contralateral Kcna2 antisense RNA was 2.2-fold greater in the injured L5 DRG than in that of the sham-operated groups, whereas the corresponding ratio for *Kcna2* mRNA was 75% lower (**Fig. 4g**). Additionally, Kcna2 protein in the ipsilateral L5 DRG was reduced by 51.8% compared to that in the contralateral L5 DRG from the sham-operated groups ($n = 12$ per group, $P < 0.05$; **Supplementary Fig. 2d**).

We further examined the opposing SNL-induced changes in Kcna2 antisense RNA and *Kcna2* mRNA in individual DRG neurons. Ratios of *Kcna2* to Kcna2 antisense RNA were approximately 82, 118 and 121 in small, medium and large DRG neurons, respectively, from sham-operated rats (**Fig. 4h**). These ratios decreased, particularly in medium and large DRG neurons, 7 d after SNL (**Fig. 4h**). Taken together, these results demonstrate that Kcna2 antisense RNA can be induced in the injured DRG after peripheral nerve injury.

MZF1 promotes Kcna2 antisense RNA gene activity after SNL

How is DRG Kcna2 antisense RNA upregulated after nerve injury? Using the online software TFSEARCH, we found a consensus binding motif ($_{-161}$AGTGGGGA$_{-154}$) for the transcriptional activator myeloid zinc finger protein 1 (MZF1) in the promoter region of the *Kcna2*

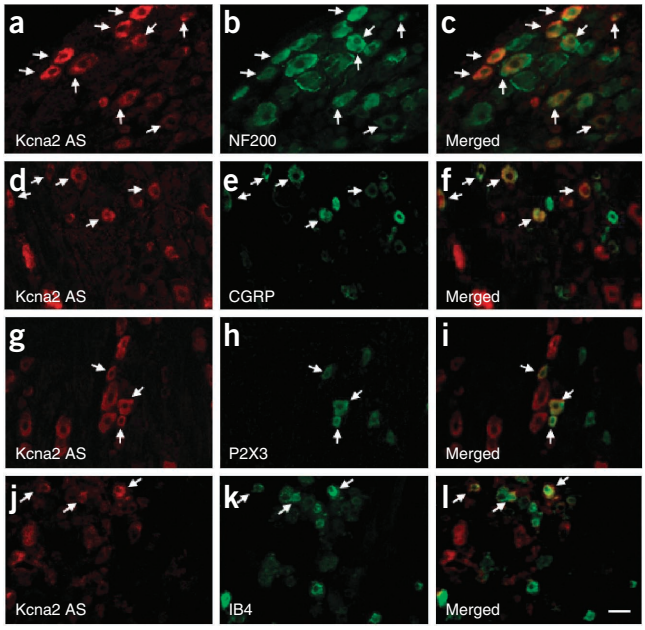

Figure 2 Subpopulation distribution of Kcna2 antisense RNA–containing neurons in DRG of naive rats. Neurons were double-labeled for Kcna2 antisense (AS) RNA and for neurofilament-200 (NF200; **a**–**c**), calcitonin gene-related peptide (CGRP; **d**–**f**), P2X3 (**g**–**i**) or isolectin B4 (IB4; **j**–**l**). Arrows, double-labeled neurons. $n = 5$ rats. Scale bar, 40 μm.

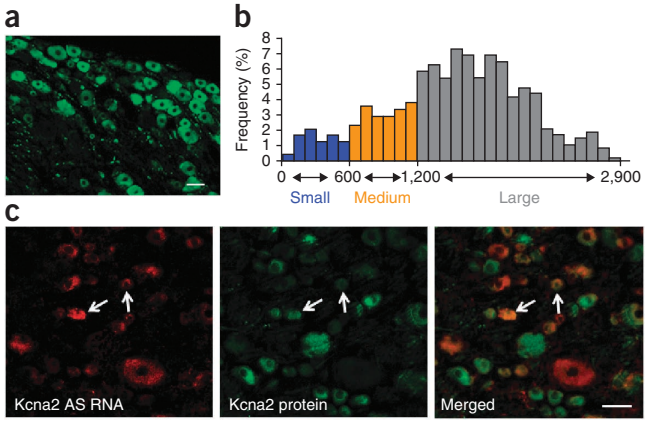

Figure 3 Distribution of Kcna2 protein and double labeling of Kcna2 antisense RNA with Kcna2 protein in normal rat DRG. (**a**) A representative example showing the distribution of Kcna2-positive neurons. Approximately 70% (855 of 1,220) of DRG neurons were positive for Kcna2. (**b**) Distribution of Kcna2-positive somata: large, 72.6%; medium, 18.6%; small, 8.6%. (**c**) Representative examples showing that most Kcna2 antisense (AS) RNA-labeled neurons in the DRG express low amounts of Kcna2 protein, although a few (arrows) display high-density Kcna2 protein staining. $n = 5$ rats. Scale bars, 50 μm.

antisense RNA gene[20,21]. An electrophoretic mobility shift assay demonstrated binding of MZF1 to this motif in the DRG (**Fig. 5a**). A chromatin immunoprecipitation assay revealed that a fragment of the *Kcna2* antisense RNA promoter that includes the binding motif could be amplified from the complex immunoprecipitated with MZF1 antibody in nuclear fractions from DRGs in sham-operated rats (**Fig. 5b**). This amplification did not occur with normal serum (**Fig. 5b**) or after preabsorption of MZF1 antibody (data not shown), indicating that the binding of MZF1 to the *Kcna2* antisense RNA promoter is specific and selective. SNL increased the binding of MZF1 to the *Kcna2* antisense gene promoter, as demonstrated by a 4.12-fold greater band density in the ipsilateral L5 DRG from SNL rats compared to that from sham-operated rats on day 14 ($n = 6$ rats per group, $P < 0.05$). This increase may result from SNL-induced time-dependent upregulation of MZF1 in the ipsilateral L5 DRG (**Fig. 5c**,**d**). As expected, neither sham nor SNL surgery altered basal binding activity or MZF1 expression in the contralateral L5 DRG and ipsilateral L4 DRG (data not shown). Moreover, *Mzf1* mRNA was expressed with Kcna2 antisense RNA in the DRG neurons (**Supplementary Fig. 3a**). These *in vivo* findings suggest that peripheral nerve injury increases DRG MZF1 expression, allowing the binding of more MZF1 to the promoter region of *Kcna2* antisense gene in the injured DRG neurons.

To further examine whether MZF1 directly regulates Kcna2 antisense RNA expression, we overexpressed full-length *Mzf1* in cultured human embryonic kidney (HEK)-293T cells (**Supplementary Fig. 3b**,**c**), which express endogenous Kcna2 antisense RNA, Kcna2 and other voltage-gated potassium channels. MZF1 overexpression significantly increased Kcna2 antisense RNA and correspondingly decreased *Kcna2* mRNA and Kcna2 protein (**Fig. 5e**,**f**). These responses were abolished in cells co-transfected with full-length *Mzf1* vector and *Mzf1*-specific short interfering RNA (but not scrambled *Mzf1* siRNA) (**Fig. 5e**,**f** and **Supplementary Fig. 3d**), indicating that upregulation of Kcna2 antisense RNA was specific

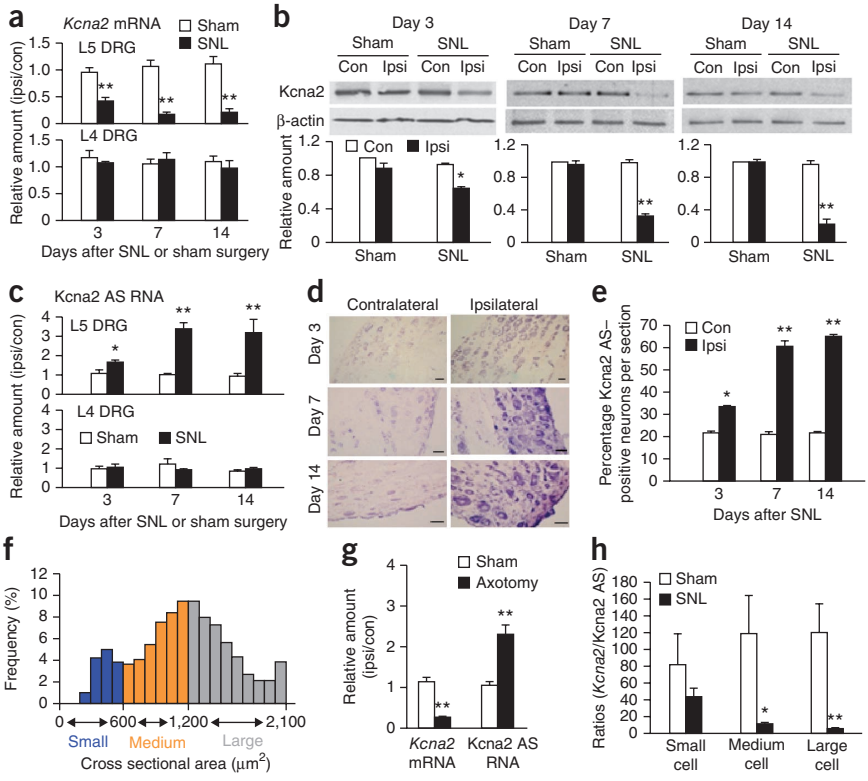

Figure 4 Changes in expression of DRG Kcna2 antisense RNA and Kcna2 after peripheral nerve injury. (**a**) *Kcna2* mRNA expression in L4/5 DRGs after SNL or sham surgery. Ipsi, ipsilateral; con, contralateral. $n = 12$ rats per group per time point. $F = 60.05$. $^{**}P < 0.01$ versus the sham-operated group at the corresponding time point. Two-way ANOVA with Tukey *post-hoc* test. (**b**) Kcna2 protein expression in L5 DRG after SNL or sham surgery. $n = 12$ rats per group per time point. $F = 6.90$ for day 3, 74.11 for day 7 and 351.39 for day 14. $^{*}P < 0.05$, $^{**}P < 0.01$ versus the contralateral side of the sham-operated group at the corresponding time point. Two-way ANOVA with Tukey *post-hoc* test. Full-length blots are presented in **Supplementary Figure 7**. (**c**) Kcna2 antisense (AS) RNA expression in L4/5 DRGs after SNL or sham surgery. $n = 12$ rats per group per time point. $F = 35.51$. $^{*}P < 0.05$, $^{**}P < 0.01$ versus the sham-operated group at the corresponding time point. Two-way ANOVA with Tukey *post-hoc* test. (**d**,**e**) Kcna2 AS RNA–positive neurons in L5 DRGs after SNL. $n = 5$ rats per time point. $F = 358.18$. $^{*}P < 0.05$, $^{**}P < 0.01$ versus the corresponding contralateral side. Scale bars, 40 μm. Two-way ANOVA with Tukey *post-hoc* test. (**f**) Histogram; 46.4% of Kcna2 AS RNA-positive neurons are large, 39.1% medium, and 14.5% small in the ipsilateral L5 DRG on day 14 after SNL. (**g**) Expression of Kcna2 AS RNA and *Kcna2* mRNA in L4/5 DRGs on day 7 after axotomy or sham surgery. $n = 12$ rats per group. $t = -14.19$ for Kcna2 AS RNA and 7.55 for mRNA. $^{**}P < 0.01$ versus the corresponding sham-operated group. Paired Student's *t*-test. (**h**) The ratios of *Kcna2* mRNA to Kcna2 AS RNA in individual DRG neurons on day 7 after SNL or sham surgery. $n = 15$ neurons per cell type per group. $t = 1.01$ for small cells, 3.35 for medium cells and 4.48 for large cells. $^{*}P < 0.05$, $^{**}P < 0.01$ versus the corresponding sham-operated group. Paired Student's *t*-test. Error bars, s.e.m.

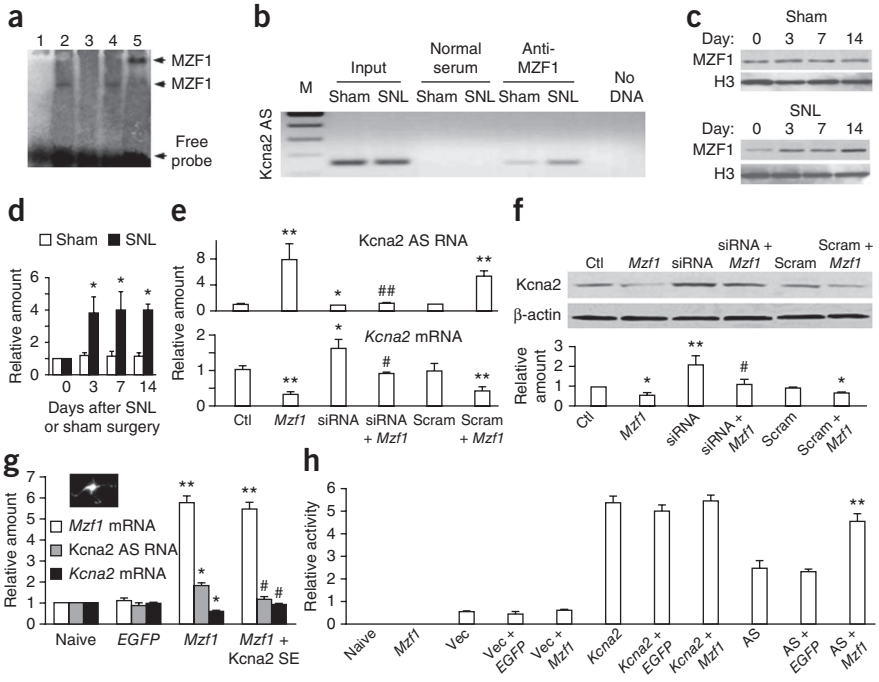

Figure 5 MZF1 mediates nerve injury–induced upregulation of DRG Kcna2 antisense RNA. (**a**) Electrophoretic mobility shift assay showing binding specificity of MZF1 for the *Kcna2* antisense promoter. Labeled probe alone (lane 1) or plus nuclear extract (lane 2), nuclear extract and 50-fold unlabeled probe (lane 3), nuclear extract and 50-fold unlabeled mutant probe (lane 4), or nuclear extract and antibody to MZF1 (lane 5). $n = 3$ repeats. (**b**) *Kcna2* antisense (AS) promoter fragments immunoprecipitated by rabbit antibody to MZF1 in the ipsilateral L5 DRGs on day 14 after SNL or sham surgery. Input, total purified fragments. M, ladder marker. (**c**,**d**) MZF1expression in the ipsilateral L5 DRGs after SNL or sham surgery. Histone H3 (H3) serves as a loading control. $n = 9$ rats per time point per group. $F = 14.13$. $^{*}P < 0.05$ versus the corresponding naive group (day 0). One-way ANOVA with Tukey *post-hoc* test. (**e**,**f**) Amounts of Kcna2 AS RNA (**e**), *Kcna2* mRNA (**e**) and Kcna2 protein (**f**) in HEK-293T cells transfected as shown. Ctl, *EGFP* control; siRNA, *Mzf1* siRNA; Scram, scrambled *Mzf1* siRNA. $n = 5$ repeats per treatment. $F = 8.53$ for AS RNA, 12.92 for mRNA and 7.93 for protein. $^{*}P < 0.05$, $^{**}P < 0.01$ versus EGFP control. $^{\#}P < 0.05$, $^{\#\#}P < 0.01$ versus *Mzf1* alone. One-way ANOVA with Tukey *post-hoc* test. (**g**) Amounts of *Mzf1* mRNA, Kcna2 AS RNA and *Kcna2* mRNA in rat DRG cultured neurons transduced as shown. Inset, an AAV5-EGFP-labeled neuron. $n = 3$ repeats per treatment. $F = 168.61$ for *Mzf1* mRNA, 30.84 for Kcna2 AS RNA and 17.79 for *Kcna2* mRNA. $^{*}P < 0.05$, $^{**}P < 0.01$ versus the corresponding naive condition. $^{\#}P < 0.05$ versus the corresponding AAV5-MZF1 alone. Two-way ANOVA with Tukey *post-hoc* test. (**h**) *Kcna2* gene promoter and *Kcna2* AS gene promoter activities in HEK-293T cells transfected as shown. Vec, control vector (pGL3-Basic). $n = 3$ repeats per treatment. $F = 82.09$. $^{**}P < 0.01$ versus pGL3-Kcna2 AS vector alone. One-way ANOVA with Tukey *post-hoc* test. Error bars, s.e.m. Full-length blots are presented in **Supplementary Figure 7**.

in response to MZF1. *Mzf1* siRNA transfection alone also reduced basal Kcna2 antisense RNA expression and increased basal expression of *Kcna2* mRNA and protein (**Fig. 5e**,**f**). We confirmed MZF1-triggered upregulation of Kcna2 antisense RNA and downregulation of *Kcna2* mRNA in cultured DRG neurons that were transduced with recombinant adeno-associated virus 5 (AAV5) that expressed full-length *Mzf1* (**Fig. 5g**).

A software prediction showed that the promoter region of the *Kcna2* gene does not contain a consensus MZF1-binding motif. MZF1 does not enhance the activity of the *Kcna2* gene promoter, but it markedly activates the *Kcna2* antisense gene promoter (**Fig. 5h**). In naive rats, *Kcna2* gene promoter fragments were not amplified from the DRG nuclear complex immunoprecipitated by MZF1 antibody (data not shown). MZF1-triggered downregulation of Kcna2 is thus not likely

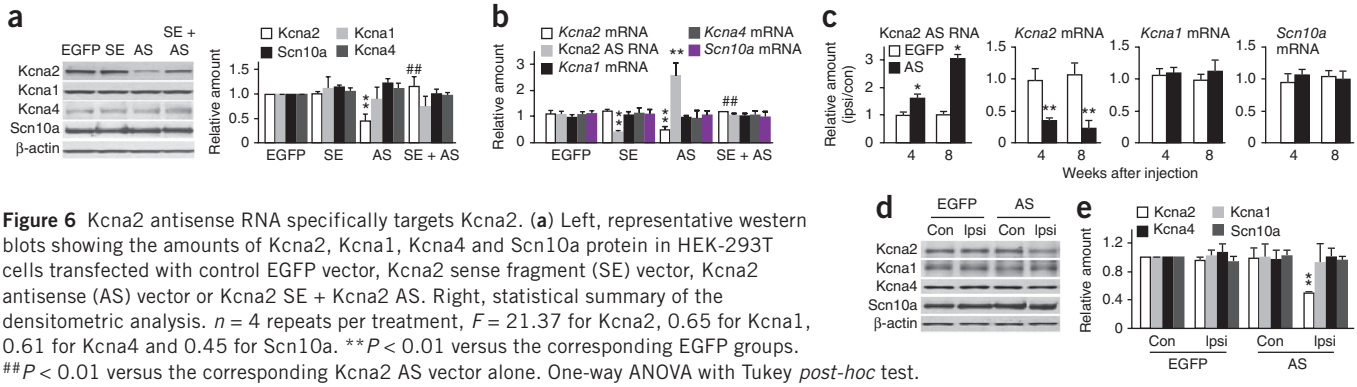

Figure 6 Kcna2 antisense RNA specifically targets Kcna2. (**a**) Left, representative western blots showing the amounts of Kcna2, Kcna1, Kcna4 and Scn10a protein in HEK-293T cells transfected with control EGFP vector, Kcna2 sense fragment (SE) vector, Kcna2 antisense (AS) vector or Kcna2 SE + Kcna2 AS. Right, statistical summary of the densitometric analysis. $n = 4$ repeats per treatment, $F = 21.37$ for Kcna2, 0.65 for Kcna1, 0.61 for Kcna4 and 0.45 for Scn10a. $^{**}P < 0.01$ versus the corresponding EGFP groups. $^{\#\#}P < 0.01$ versus the corresponding Kcna2 AS vector alone. One-way ANOVA with Tukey *post-hoc* test. (**b**) Amounts of Kcna2 AS RNA and of mRNAs for various ion channels in rat DRG cultured neurons transduced with AAV5-EGFP, AAV5-Kcna2 SE, AAV5-Kcna2 AS or AAV5-Kcna2 SE + AAV5-Kcna2 AS. $n = 3$ repeats per treatment. $F = 10.06$ for *Kcna2* mRNA, 11.90 for Kcna2 AS RNA, 0.24 for *Kcna1* mRNA, 0.65 for *Kcna4* mRNA and 0.87 for *Scn10a* mRNA. $^{**}P < 0.01$ versus AAV5-EGFP alone. $^{\#\#}P < 0.01$ versus the corresponding AAV5-Kcna2 AS alone. One-way ANOVA with Tukey *post-hoc* test. (**c**) Levels of Kcna2 AS RNA and mRNAs for various ion channels in the ipsilateral (ipsi) and contralateral (con) L4/5 DRGs 4 and 8 weeks after injection with AAV5-EGFP or AAV5-Kcna2 AS. $n = 12$ rats per treatment. $F = 15.91$ for Kcna2 AS RNA, 20.45 for *Kcna2* mRNA, 0.39 for *Kcna1* mRNA and 0.56 for *Scn10a* mRNA. $^{*}P < 0.05$, $^{**}P < 0.01$ versus the corresponding EGFP-treated group. Two-way ANOVA with Tukey *post-hoc* test. (**d**) Representative western blots of ipsilateral and contralateral L4/5 DRGs 8 weeks after injection with AAV5-EGFP or AAV5-Kcna2 AS. (**e**) Statistical summary of the densitometric analysis. $n = 10$ rats per group. $F = 15.51$ for Kcna2, 0.35 for Kcna1, 0.78 for Kcna4 and 0.48 for Scn10a. $^{**}P < 0.01$ versus corresponding contralateral sides of the AAV5-EGFP-treated group. One-way ANOVA with Tukey *post-hoc* test. Error bars, s.e.m. Full-length blots are presented in **Supplementary Figure 7**.

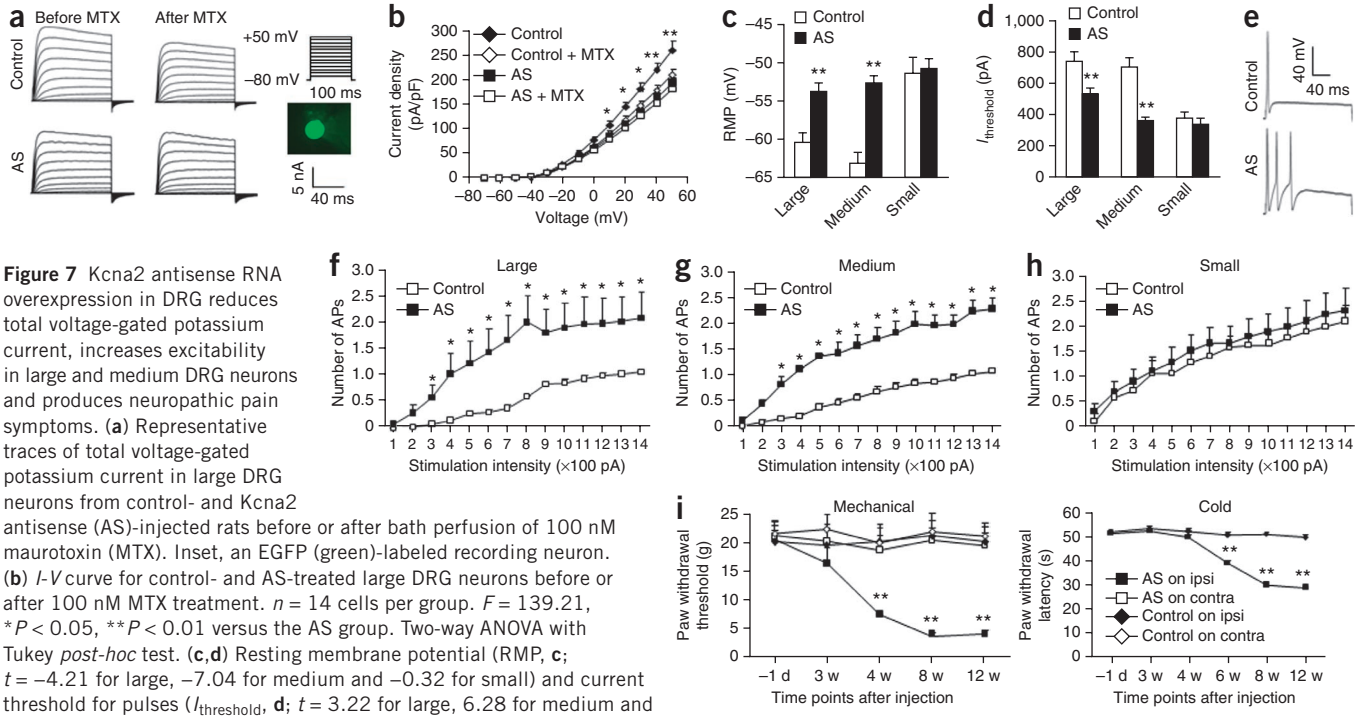

Figure 7 Kcna2 antisense RNA overexpression in DRG reduces total voltage-gated potassium current, increases excitability in large and medium DRG neurons and produces neuropathic pain symptoms. (**a**) Representative traces of total voltage-gated potassium current in large DRG neurons from control- and Kcna2 antisense (AS)-injected rats before or after bath perfusion of 100 nM maurotoxin (MTX). Inset, an EGFP (green)-labeled recording neuron. (**b**) *I-V* curve for control- and AS-treated large DRG neurons before or after 100 nM MTX treatment. $n = 14$ cells per group. $F = 139.21$, $^*P < 0.05$, $^{**}P < 0.01$ versus the AS group. Two-way ANOVA with Tukey *post-hoc* test. (**c**,**d**) Resting membrane potential (RMP, **c**; $t = -4.21$ for large, -7.04 for medium and -0.32 for small) and current threshold for pulses ($I_{threshold}$, **d**; $t = 3.22$ for large, 6.28 for medium and 0.73 for small). $n = 33$ large, 42 medium and 30 small cells from the control group (12 rats). $n = 43$ large, 70 medium and 32 small cells from the AS group (14 rats). $^{**}P < 0.01$ versus the corresponding control group. Unpaired Student's *t*-test. (**e**) Representative traces of the evoked action potentials (AP) in DRG neurons. (**f**–**h**) Numbers of evoked APs from control- and AS-injected rats after application of different currents. Numbers of cells recorded same as in **c**. $F = 18.45$ for large, 20.65 for medium and 0.67 for small cells. $^*P < 0.05$ versus the same stimulation intensity in the control group. Two-way ANOVA with Tukey *post-hoc* test. (**i**) Ipsilateral (ipsi) and contralateral (contra) paw withdrawal responses to mechanical ($F = 38.31$) and cold ($F = 65.77$) stimuli from control and AS-injected rats; w, weeks. $n = 14$ rats per group. $^{**}P < 0.01$ versus control on the ipsilateral side at the corresponding time points. Two-way ANOVA with Tukey *post-hoc* test. Error bars, s.e.m.

to occur by direct binding of MZF1 to the *Kcna2* gene promoter. To examine whether Kcna2 antisense RNA mediates this effect, we cloned an AAV5 vector that expresses a Kcna2 sense RNA fragment (−311 to +40). This fragment significantly blocked Kcna2 antisense RNA expression (**Fig. 6a**,**b**) but did not alter basal expression of *Kcna2* mRNA or Kcna2 protein or produce truncated Kcna2 protein in cultured HEK-293T cells or DRG neurons (**Fig. 6a**,**b**). We found that the Kcna2 sense fragment blocked the MZF1-induced increase in Kcna2 antisense RNA and reversed the MZF1-induced reduction in *Kcna2* mRNA in DRG neurons (**Fig. 5g**). Thus, MZF1-induced Kcna2 downregulation may be attributable to MZF1-triggered *Kcna2* antisense gene expression.

DRG Kcna2 antisense RNA leads to neuropathic pain symptoms

We next investigated whether mimicking nerve injury–induced upregulation of DRG Kcna2 antisense RNA alters DRG Kcna2 expression and function, DRG neuronal excitability and nociceptive thresholds. To this end, we transfected Kcna2 antisense RNA proviral vector or control EGFP vector into cultured HEK-293T cells and transduced AAV5 that expressed Kcna2 antisense RNA (AAV5-Kcna2 antisense) or EGFP (AAV5-EGFP) into cultured DRG neurons. Kcna2 antisense RNA markedly decreased Kcna2 mRNA and protein expression, but not *Kcna1*, *Kcna4* or *Scn10a* expression (**Fig. 6a**,**b**). Then we injected AAV5–Kcna2 antisense or AAV5-EGFP unilaterally into the L4 and L5 (L4/5) DRGs. Four weeks after injection, EGFP-labeled AAV5 was limited to the ipsilateral L4/5 DRG neurons and their fibers and terminals (**Supplementary Fig. 4a–g**). Approximately 87.1% of labeled cells were positive for NF-200, 4.21% for substance P, 6.32% for CGRP and 10.0% for P2X3 (**Supplementary Fig. 4h**), a distribution similar to that of Kcna2 antisense RNA–positive neurons in the injured DRG after SNL (**Fig. 4f**). Expression of the Kcna2 antisense RNA was significantly increased in the L4/5 DRGs at 4 weeks, reached a peak at 8 weeks and remained high for at least 12 weeks after viral injection (**Fig. 6c**). In contrast, the expression of *Kcna2* mRNA and protein was significantly and temporally reduced in the ipsilateral L4/5 DRGs (**Fig. 6c–e**). The amounts of mRNA and protein of *Kcna1*, *Kcna4* or *Scn10a* were unaffected (**Fig. 6c–e**). These results indicate that Kcna2 antisense RNA specifically and selectively targets Kcna2.

Using a voltage-clamp technique, we recorded Kcna2-related current in neurons freshly dissociated from the injected L4/5 DRGs 8–12 weeks after injection. To increase the recording efficiency, we injected AAV5-EGFP alone (control group) or a mixed viral solution of AAV5-Kcna2 antisense plus AAV5-EGFP (Kcna2 antisense-treated group) and recorded only green DRG neurons (**Fig. 7a**). In the Kcna2 antisense-treated group, total voltage-gated potassium current density was significantly lower in large- and medium-diameter neurons (**Fig. 7a**,**b** and **Supplementary Fig. 5a–c**). To verify whether this reduction was due to Kcna2 downregulation, we used bath application of 100 nM maurotoxin (MTX), a selective Kcna2 current inhibitor[22–24]. MTX produced greater reductions in total voltage-gated potassium current in large ($n = 14$ per group) and medium (control: $n = 17$; antisense, $n = 15$) neurons from the control group than in those from the Kcna2 antisense–treated group at depolarized voltages ($P < 0.05$ or 0.01; **Fig. 7a**,**b** and **Supplementary Fig. 5a–c**). When tested at +50 mV, large and medium neurons in the control group retained 81.7 ± 1.7% and 85.1 ± 2.2% of current, respectively, after MTX treatment, but large and medium neurons from the Kcna2 antisense–treated group retained 92.3 ± 0.9% and 94.9 ± 1.6% of current,

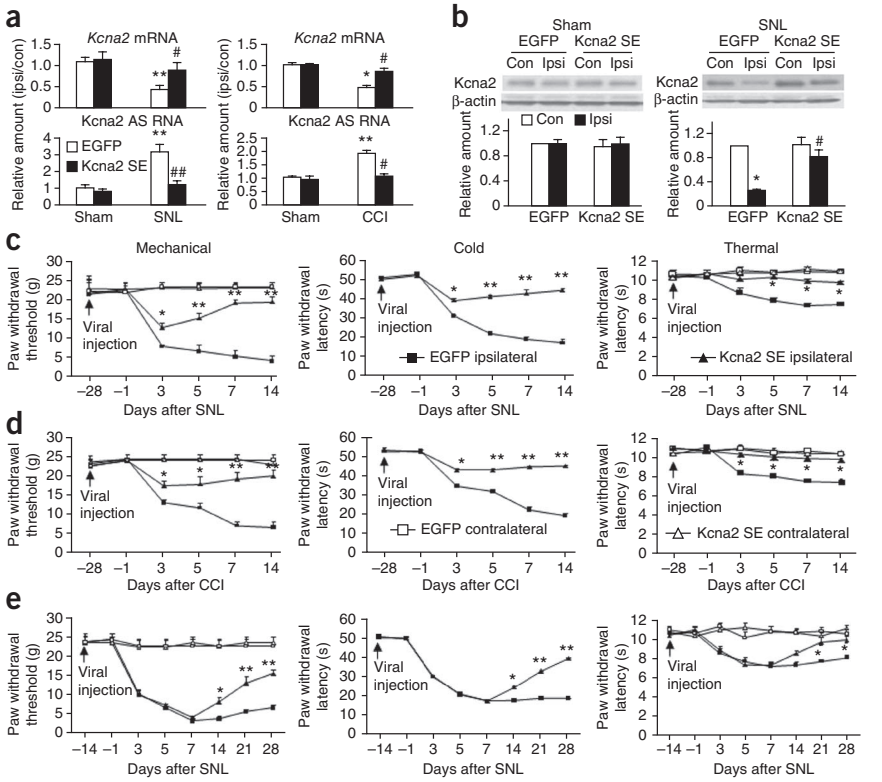

Figure 8 Blocking nerve injury–induced upregulation of DRG Kcna2 antisense RNA attenuates neuropathic pain. (**a**) *Kcna2* mRNA and Kcna2 antisense (AS) RNA expression in the ipsilateral (Ipsi) and contralateral (Con) L5 DRGs on day 14 after SNL ($F = 41.03$ for AS RNA and 10.26 for mRNA), CCI ($F = 35.91$ for AS RNA and 8.73 for mRNA) or sham surgery in the EGFP-treated and Kcna2 sense fragment (Kcna2 SE)-treated groups. $n = 12$ rats per group. $^{**}P < 0.01$ versus the EGFP-treated group after sham surgery. $^{\#}P < 0.05$, $^{\#\#}P < 0.01$ versus the corresponding EGFP-treated group after SNL or CCI. Two-way ANOVA with Tukey *post-hoc* test. (**b**) Kcna2 protein expression in the ipsilateral and contralateral L5 DRGs on day 14 after sham surgery or SNL in the EGFP-treated and Kcna2 SE–treated groups. $n = 8$ rats per group. $F = 9.26$ in SNL and 0.53 in sham-operated. $^{*}P < 0.05$ versus corresponding contralateral side of the EGFP-treated group. $^{\#}P < 0.05$ versus the corresponding ipsilateral side of the EGFP-treated group. Two-way ANOVA with Tukey *post-hoc* test. Full-length blots are presented in **Supplementary Figure 7**. (**c**,**d**) Effect of Kcna2 SE on the development of SNL- or CCI-induced pain hypersensitivities. Paw withdrawal responses at the times shown before and after SNL ($F = 23.25$ for mechanical, 545.13 for cold and 15.31 for thermal) or CCI ($F = 22.51$ for mechanical, 267.42 for cold and 12.45 for thermal). $n = 8$ rats per group. $^{*}P < 0.05$, $^{**}P < 0.01$ versus the ipsilateral side of the EGFP-treated group at the corresponding time point. Two-way ANOVA with Tukey *post-hoc* test. (**e**) Effect of Kcna2 SE on the maintenance of SNL-induced pain hypersensitivities. Paw withdrawal responses at the times shown before and after SNL ($F = 22.66$ for mechanical, 104.16 for cold and 7.64 for thermal). $n = 8$ rats per group. $^{*}P < 0.05$, $^{**}P < 0.01$ versus the ipsilateral side of the EGFP-treated group at the corresponding time point. Two-way ANOVA with Tukey *post-hoc* test. Error bars, s.e.m.

respectively. In small DRG neurons, the current reduction by MTX was less prominent, but the difference between control and Kcna2 antisense–treated groups was still significant ($n = 11$ neurons per group, $P < 0.05$; **Supplementary Fig. 5d–f**). These data indicate that Kcna2 antisense RNA reduces total voltage-gated potassium current densities in large and medium DRG neurons and decreases Kcna2-related current in all DRG neurons.

To assess whether Kcna2 antisense RNA modulates DRG neuronal excitability, we carried out whole-cell current-clamp recording 8–12 weeks after injection. Compared to the control group, Kcna2 antisense RNA treatment significantly increased resting membrane potentials, by 6.74 mV and 10.52 mV in large and medium neurons, respectively (**Fig. 7c**), and reduced current thresholds by 217 pA and 344 pA, respectively ($P < 0.01$; **Fig. 7d**). The average number of action potentials evoked by stimulation of ≥300 pA in the Kcna2 antisense–treated group was greater than the average number evoked by the corresponding stimulation intensity in the control group in large and medium neurons (**Fig. 7e–g**). No such changes were observed in small DRG neurons (**Fig. 7c**,**d**,**h**). There were no apparent differences between the two groups in membrane input resistances or other action potential parameters, such as amplitude, threshold, duration, overshoot and after-hyperpolarization amplitude (**Supplementary Table 1**). Application of MTX into DRG neurons produced similar effects (**Supplementary Fig. 6** and **Supplementary Table 1**). Our findings indicate that Kcna2 knockdown or current inhibition increases DRG neuronal excitability.

Lastly, we examined whether rats that received L4/5 DRG injections of Kcna2 antisense RNA showed behavioral changes in nociceptive thresholds. Injection of AAV5–Kcna2 antisense, but not of AAV5-EGFP, produced mechanical and cold hypersensitivities as demonstrated by ipsilateral decreases in paw withdrawal threshold and paw withdrawal latency, respectively ($n = 14$ rats per group, $P < 0.01$; **Fig. 7i**). These hypersensitivities developed by 4 to 6 weeks, reached a peak at 8 weeks and were maintained for at least 12 weeks (**Fig. 7i**). Neither AAV5-Kcna2 antisense nor AAV5-EGFP affected locomotor functions (data not shown). These findings suggest that Kcna2 antisense RNA–triggered DRG Kcna2 downregulation induces mechanical and cold hypersensitivities, two main clinical symptoms of neuropathic pain.

Blocking DRG Kcna2 antisense RNA attenuates neuropathic pain

Finally, we inquired whether blocking nerve injury–induced upregulation of DRG Kcna2 antisense RNA would affect reductions in DRG Kcna2 expression and nociceptive thresholds after nerve injury. Consistent with our *in vitro* work (**Fig. 6a**,**b**), *in vivo* DRG injection of AAV5–Kcna2 sense fragment, but not AAV5-EGFP, significantly blocked upregulation of Kcna2 antisense RNA and downregulation of *Kcna2* mRNA and protein in the injured DRGs after SNL or chronic constriction injury (CCI) (**Fig. 8a**,**b**). These effects occurred at 4 weeks and were maintained for at least 12 weeks after viral injection. Injection of AAV5–Kcna2 sense fragment alone did not alter basal expression of *Kcna2* mRNA and Kcna2 protein or Kcna2 antisense RNA in the ipsilateral L5 DRG of sham-operated rats (**Fig. 8a**,**b**). To examine the role of Kcna2 antisense RNA in neuropathic pain induction, we subjected rats to SNL 4 weeks after DRG viral injection, as our pilot work showed that there was too little Kcna2 sense fragment to block SNL-induced Kcna2 antisense RNA expression before that time. SNL produced mechanical, cold and thermal hypersensitivities on

the ipsilateral side in the EGFP-injected group (**Fig. 8c**). By contrast, hypersensitivity was attenuated in the Kcna2 sense fragment–injected rats (**Fig. 8c**). Paw withdrawal threshold to mechanical stimulation and paw withdrawal latency to cold and thermal stimuli were higher in the Kcna2 sense fragment–injected rats than in the EGFP-injected group from days 3 to 14 after SNL (**Fig. 8c**). We observed similar effects of AAV5-Kcna2 sense fragment on neuropathic pain development in the CCI model as well (**Fig. 8d**).

To further investigate the role of Kcna2 antisense RNA in neuropathic pain maintenance, we subjected rats to SNL 2 weeks after DRG viral injection. Mechanical, cold and thermal hypersensitivities were completely developed in both the Kcna2 sense fragment–injected and EGFP-injected rats on day 7 after SNL (**Fig. 8e**). These hypersensitivities were markedly attenuated on days 14, 21 and 28 after SNL in the Kcna2 sense fragment–injected rats (**Fig. 8e**). Neither AAV5–Kcna2 sense fragment nor AAV5-EGFP affected paw withdrawal threshold or latency on the contralateral side (**Fig. 8c–e**), affected locomotor function (data not shown) or altered basal responses to mechanical or cold stimuli in sham-operated rats (data not shown). Our findings indicate that Kcna2 antisense RNA contributes to neuropathic pain development and maintenance and that blocking its expression may have clinical applications in neuropathic pain treatment.

DISCUSSION

lncRNAs were recently shown to occur naturally in mammals[18,19]. They can be transcribed in *cis* from the opposing DNA strands of the RNA genes at the same genomic locus or in *trans* from a locus different from that of the RNA genes[25]. Rat Kcna2 antisense RNA is more than 2.5 kb and complementary to most of the *Kcna2* RNA sequence, strongly suggesting that Kcna2 antisense RNA is a *cis*-encoded lncRNA. Of note, the Kcna2 antisense RNA exhibits the same splicing patterns as the *Kcna2* sense RNA. Because the splice junctions of the *Kcna2* sense gene are canonical (that is, they follow the GT-AG rule), splicing mechanisms of the Kcna2 antisense gene are unusual and merit further investigation.

Expression of native Kcna2 antisense RNA, like that of the mRNA, can be regulated by transcriptional activation. Nerve injury–induced upregulation of Kcna2 antisense RNA was triggered through DRG MZF1 activation. Whether other transcription factors also trigger activation of Kcna2 antisense transcription is unknown. Additionally, the increase in antisense RNA might be caused by increases in RNA stability and/or other epigenetic modification. These possibilities cannot be excluded and will be addressed in our future studies.

Kcna2 antisense RNA functions as a biologically active regulator of *Kcna2* mRNA in primary afferent neurons. Normally, Kcna2 antisense RNA was expressed at a low level in a few (mostly medium-sized) DRG neurons, whereas Kcna2 protein was highly expressed in most medium- or large-sized DRG neurons[9]. Of note, injury to the peripheral nerve not only increased Kcna2 antisense RNA expression but also altered its subpopulation distribution pattern to large- and medium-sized neurons in the injured DRG. Conversely, *Kcna2* mRNA and Kcna2 protein were correspondingly downregulated in these neurons[5–10]. This downregulation is likely caused by the increase in Kcna2 antisense RNA, as overexpression of Kcna2 antisense RNA in cultured HEK-293T cells or DRG neurons selectively and specifically inhibited *Kcna2* mRNA and protein expression. This effect may be related to the extensive overlap of their complementary regions, including the transcription and translation initiation sites. DRG Kcna subunits are functional heteromultimers[9,26–28]. The expression of other Kcna subunits was unaffected, likely because they lack complementary sequences and the inhibitory effect of Kcna2 antisense RNA occurs before the formation of heteromultimers. However, the fact that Kcna2 downregulation markedly reduced total voltage-gated potassium current density in large and medium DRG neurons indicates that Kcna2 is a key subunit in determining voltage-gated potassium channel function in these neurons. Minimal reduction was observed in small DRG neurons, possibly because Kcna2 is poorly expressed in those neurons[9].

We found that selective reduction of Kcna2 expression in DRG by Kcna2 antisense RNA decreased total voltage-gated potassium current, depolarized the resting membrane potential, decreased current threshold for activation of action potentials and increased the number of action potentials in large and medium DRG neurons. Depolarization of DRG neuronal resting membrane potential by DRG Kcna2 downregulation was also reported previously[29,30]. Kcna2 antisense RNA did not affect action potential threshold or amplitude in DRG neurons, as these two parameters may be determined predominantly by Na^+ channels. Kcna2 knockdown by Kcna2 antisense RNA produced a modest, but insignificant, increase in DRG neuronal membrane input resistances, an observation that is consistent with the fact that membrane input resistance also depends on other voltage-gated potassium channels (for example, Kcna1, Kcna4), hyperpolarization-activated cyclic nucleotide-gated channels[31,32] and chloride channels[33] expressed on DRG neuronal membrane. In addition, the depolarized resting membrane potential by itself may increase resting potassium conductance[31,32], which may counteract Kcna2 deficiency-induced increase in membrane input resistance. The increase in membrane input resistance caused by blocking voltage-gated potassium current in DRG neurons was observed only in the absence of a significant resting membrane potential depolarization[34]. The fact membrane input resistance is unchanged but that resting membrane potentials are markedly depolarized in DRG neurons has been reported after peripheral nerve injury[35].

Nerve injury-induced increases in spontaneous ectopic activity, which have been found primarily in injured myelinated afferents and the corresponding large and medium DRG neuronal bodies[36,37], are considered to play a leading role in the genesis of neuropathic pain[1,3]. Peripheral nerve injury increased Kcna2 antisense RNA mainly in medium and large DRG neurons. Kcna2 antisense RNA–induced depolarization of the resting membrane potential of DRG neurons may render those neurons more prone to hyperexcitability. Indeed, animals that overexpressed Kcna2 antisense RNA exhibited significant hypersensitivities to mechanical and noxious cold stimuli. Substance P and CGRP in the injured myelinated fibers and in large and medium DRG neurons are markedly increased as early as 2 d after nerve injury[3,38]. It is very likely that the increase in excitability of large and medium DRG neurons drives the release of these neurotransmitters from their primary afferent terminals and leads to spinal central sensitization, which contributes to the development and maintenance of neuropathic pain. This conclusion is supported by the fact that blocking SNL-evoked upregulation of Kcna2 antisense RNA reversed the reduction in DRG Kcna2 and attenuated induction and maintenance of nerve injury–induced mechanical and cold hypersensitivities. It is still a puzzle how blocking SNL-induced downregulation of DRG Kcna2 almost abolishes SNL-induced pain hypersensitivity at the late time points. We think that blocking DRG Kcna2 downregulation causes persistent reduction in DRG excitability that may enhance the decrease in primary afferent transmitter release, resulting in attenuation of spinal central sensitization formation. Persistent reduction in DRG neuronal excitability may also block further SNL-induced changes in the expression of other DRG genes, including transcription factors that govern gene expression. This activity could create positive feedback to further reduce DRG excitability.

These potential mechanisms remain to be confirmed. Taken together, our findings suggest that Kcna2 antisense RNA is an endogenous trigger in neuropathic pain development and maintenance. Regulation of Kcna2 channel expression may be a target for treating neuropathic pain.

In summary, identification of Kcna2 antisense RNA may point to regulation of Kcna2 channel expression and neuronal excitability, a novel mechanism in neuropathic pain, and potential targets for the development of therapies of this disorder. Because Kcna2 antisense RNA, *Kcna2* mRNA and Kcna2 protein are expressed broadly, they may be implicated in other pathological processes. In addition, demonstration of Kcna2 antisense RNA may challenge current molecular methodologies. For example, we cannot use sense probes usually designed as negative controls, as they detect endogenous antisense RNAs in *in situ* hybridization, or oligo(dT) primers, as they allow reverse transcription of both sense and antisense RNAs. Therefore, our findings not only provide conceptual advances regarding the development of neuropathic pain but also will affect the conduct of research in other fields.

METHODS

Methods and any associated references are available in the online version of the paper.

Note: Supplementary information is available in the online version of the paper.

ACKNOWLEDGMENTS

We thank R.J. Samulski (University of North Carolina) for the rAAV5 plasmid, J. Zhou (Institute of Biochemistry of Cell Biology, Chinese Academy of Sciences) for the full-length EGFP-MZF1 plasmid and D.Y.H. Tuan (Georgia Health Sciences University) for MZF1 antibody. We thank C.F. Levine for editorial assistance. This work was supported by the Howard Hughes Medical Institute and US National Institutes of Health (NIH) grants (NS054791 and GM087369) to X.D., by NIH grants (MH084691 and GM078579) to M.L. and by NIH grants (DA033390, NS072206) and the grants from the Rita Allen Foundation to Y.-X.T.

AUTHOR CONTRIBUTIONS

Y.-X.T. conceived the project and supervised most experiments. X.Z., Z.T., H.Z., F.E.A., J.-Y.Z., Y.-J.G., H.C., M.L., X.D. and Y.-X.T. designed the project. X.Z., F.E.A., J.-Y.Z., L.L., W.W., X.G., S.-C.K. and V.T. performed molecular, biochemical and behavioral experiments. Z.T. and X.D. performed current-clamp experiments. H.Z. and M.L. performed voltage-clamp experiments. P.N.H. did microinjection. X.Z., Z.T., H.Z., F.E.A., J.-Y.Z. L.L., W.W., X.G., V.T. and Y.-X.T. analyzed the data. Y.-X.T. wrote the manuscript. All authors read and discussed the manuscript.

COMPETING FINANCIAL INTERESTS

The authors declare no competing financial interests.

1. Campbell, J.N. & Meyer, R.A. Mechanisms of neuropathic pain. *Neuron* **52**, 77–92 (2006).
2. Chung, J.M. & Chung, K. Importance of hyperexcitability of DRG neurons in neuropathic pain. *Pain Pract.* **2**, 87–97 (2002).
3. Devor, M. Ectopic discharge in Aβ afferents as a source of neuropathic pain. *Exp. Brain Res.* **196**, 115–128 (2009).
4. Costigan, M., Scholz, J. & Woolf, C.J. Neuropathic pain: a maladaptive response of the nervous system to damage. *Annu. Rev. Neurosci.* **32**, 1–32 (2009).
5. Everill, B. & Kocsis, J.D. Nerve growth factor maintains potassium conductance after nerve injury in adult cutaneous afferent dorsal root ganglion neurons. *Neuroscience* **100**, 417–422 (2000).
6. Ishikawa, K., Tanaka, M., Black, J.A. & Waxman, S.G. Changes in expression of voltage-gated potassium channels in dorsal root ganglion neurons following axotomy. *Muscle Nerve* **22**, 502–507 (1999).
7. Kim, D.S., Choi, J.O., Rim, H.D. & Cho, H.J. Downregulation of voltage-gated potassium channel alpha gene expression in dorsal root ganglia following chronic constriction injury of the rat sciatic nerve. *Brain Res. Mol. Brain Res.* **105**, 146–152 (2002).
8. Park, S.Y. *et al.* Downregulation of voltage-gated potassium channel alpha gene expression by axotomy and neurotrophins in rat dorsal root ganglia. *Mol. Cells* **16**, 256–259 (2003).
9. Rasband, M.N. *et al.* Distinct potassium channels on pain-sensing neurons. *Proc. Natl. Acad. Sci. USA* **98**, 13373–13378 (2001).
10. Yang, E.K., Takimoto, K., Hayashi, Y., de Groat, W.C. & Yoshimura, N. Altered expression of potassium channel subunit mRNA and alpha-dendrotoxin sensitivity of potassium currents in rat dorsal root ganglion neurons after axotomy. *Neuroscience* **123**, 867–874 (2004).
11. Chabal, C., Jacobson, L., Russell, L.C. & Burchiel, K.J. Pain responses to perineuromal injection of normal saline, gallamine, and lidocaine in humans. *Pain* **36**, 321–325 (1989).
12. Chien, L.Y., Cheng, J.K., Chu, D., Cheng, C.F. & Tsaur, M.L. Reduced expression of A-type potassium channels in primary sensory neurons induces mechanical hypersensitivity. *J. Neurosci.* **27**, 9855–9865 (2007).
13. Devor, M. Potassium channels moderate ectopic excitability of nerve-end neuromas in rats. *Neurosci. Lett.* **40**, 181–186 (1983).
14. Targ, E.F. & Kocsis, J.D. Action potential characteristics of demyelinated rat sciatic nerve following application of 4-aminopyridine. *Brain Res.* **363**, 1–9 (1986).
15. Costa, F.F. Non-coding RNAs, epigenetics and complexity. *Gene* **410**, 9–17 (2008).
16. Faghihi, M.A. & Wahlestedt, C. Regulatory roles of natural antisense transcripts. *Nat. Rev. Mol. Cell Biol.* **10**, 637–643 (2009).
17. Ponting, C.P., Oliver, P.L. & Reik, W. Evolution and functions of long noncoding RNAs. *Cell* **136**, 629–641 (2009).
18. Gibb, E.A., Brown, C.J. & Lam, W.L. The functional role of long non-coding RNA in human carcinomas. *Mol. Cancer* **10**, 38 (2011).
19. Wapinski, O. & Chang, H.Y. Long noncoding RNAs and human disease. *Trends Cell Biol.* **21**, 354–361 (2011).
20. Hsieh, Y.H. *et al.* PKCα expression regulated by Elk-1 and MZF-1 in human HCC cells. *Biochem. Biophys. Res. Commun.* **339**, 217–225 (2006).
21. Luo, X., Zhang, X., Shao, W., Yin, Y. & Zhou, J. Crucial roles of MZF-1 in the transcriptional regulation of apomorphine-induced modulation of FGF-2 expression in astrocytic cultures. *J. Neurochem.* **108**, 952–961 (2009).
22. Fulton, S. *et al.* Contribution of Kv1.2 voltage-gated potassium channel to D2 autoreceptor regulation of axonal dopamine overflow. *J. Biol. Chem.* **286**, 9360–9372 (2011).
23. Castle, N.A. *et al.* Maurotoxin: a potent inhibitor of intermediate conductance Ca2+-activated potassium channels. *Mol. Pharmacol.* **63**, 409–418 (2003).
24. Visan, V., Fajloun, Z., Sabatier, J.M. & Grissmer, S. Mapping of maurotoxin binding sites on hKv1.2, hKv1.3, and hIKCa1 channels. *Mol. Pharmacol.* **66**, 1103–1112 (2004).
25. Lavorgna, G. *et al.* In search of antisense. *Trends Biochem. Sci.* **29**, 88–94 (2004).
26. Rehm, H. & Tempel, B.L. Voltage-gated K+ channels of the mammalian brain. *FASEB J.* **5**, 164–170 (1991).
27. Robbins, C.A. & Tempel, B.L. Kv1.1 and Kv1.2: similar channels, different seizure models. *Epilepsia* **53** (suppl. 1), 134–141 (2012).
28. Vacher, H. & Trimmer, J.S. Diverse roles for auxiliary subunits in phosphorylation-dependent regulation of mammalian brain voltage-gated potassium channels. *Pflugers Arch.* **462**, 631–643 (2011).
29. Dodson, P.D., Barker, M.C. & Forsythe, I.D. Two heteromeric Kv1 potassium channels differentially regulate action potential firing. *J. Neurosci.* **22**, 6953–6961 (2002).
30. Luo, J.-L. *et al.* Enhanced excitability and down-regulated voltage-gated potassium channels in colonic DRG neurons from neonatal maternal separation rats. *J. Pain* **12**, 600–609 (2011).
31. Cardenas, C.G. *et al.* Serotonergic modulation of hyperpolarization-activated current in acutely isolated rat dorsal root ganglion neurons. *J. Physiol. (Lond.)* **518**, 507–523 (1999).
32. Zheng, Q. *et al.* Enhanced excitability of small dorsal root ganglion neurons in rats with bone cancer pain. *Mol. Pain* **8**, 24 (2012).
33. Rinke, I., Artmann, J. & Stein, V. ClC-2 voltage-gated channels constitute part of the background conductance and assist chloride extrusion. *J. Neurosci.* **30**, 4776–4786 (2010).
34. Nicol, G.D., Vasko, M.R. & Evans, A.R. Prostaglandins suppress an outward potassium current in embryonic rat sensory neurons. *J. Neurophysiol.* **77**, 167–176 (1997).
35. Kim, Y.I. *et al.* Cell type-specific changes of the membrane properties of peripherally-axotomized dorsal root ganglion neurons in a rat model of neuropathic pain. *Neuroscience* **86**, 301–309 (1998).
36. Liu, C.N. *et al.* Tactile allodynia in the absence of C-fiber activation: altered firing properties of DRG neurons following spinal nerve injury. *Pain* **85**, 503–521 (2000).
37. Tal, M., Wall, P.D. & Devor, M. Myelinated afferent fiber types that become spontaneously active and mechanosensitive following nerve transection in the rat. *Brain Res.* **824**, 218–223 (1999).
38. Weissner, W., Winterson, B.J., Stuart-Tilley, A., Devor, M. & Bove, G.M. Time course of substance P expression in dorsal root ganglia following complete spinal nerve transection. *J. Comp. Neurol.* **497**, 78–87 (2006).

ONLINE METHODS

Animals. Male Sprague-Dawley rats weighing 200–250 g were kept in a standard 12-h light/dark cycle, with water and food pellets available *ad libitum*. All procedures used were approved by the Animal Care and Use Committee at the Johns Hopkins University and consistent with the ethical guidelines of the US National Institutes of Health and the International Association for the Study of Pain. All efforts were made to minimize animal suffering and to reduce the number of animals used. All of the experimenters were blind to treatment condition.

Nerve injury models. L5 spinal nerve ligation (SNL)[39–41], chronic constriction injury (CCI)[42] and sciatic nerve axotomy[39] models of neuropathic pain were carried out as described previously. Sham-operated groups underwent identical procedures but without transection of the respective nerve.

Behavioral analysis. Mechanical, cold, thermal and locomotor behavioral tests were carried out. Each behavioral test was carried out at 1-h intervals. Paw withdrawal thresholds in response to mechanical stimuli were first measured with the up–down testing paradigm as described previously[39]. Paw withdrawal latencies to noxious cold (0 °C) were then measured with a cold plate, the temperature of which was monitored continuously. Each animal was placed in a Plexiglas chamber on the cold plate, which was set at 0 °C. The length of time between the placement of the hind paw on the plate and the animal jumping, with or without paw licking and flinching, was defined as the paw withdrawal latency. Each trial was repeated three times at 10-min intervals for the paw on the ipsilateral side. A cutoff time of 60 s was used to avoid tissue damage. Finally, paw withdrawal latencies to noxious heat were measured with Model 336 Analgesia Meter (IITC Inc./Life Science Instruments, Woodland Hills, CA, USA) as described previously[41]. Tests of locomotor function, including placing, grasping and righting reflexes, were performed before and after viral injection according to previously described protocols[39,40,43].

Cell line culture and transfection. HEK-293T cells were cultured in Dulbecco's modified Eagle's medium at 37 °C in a humidified incubator with 5% CO_2. The plasmids were transfected into the HEK-293T cells with Lipofectamine 2000 (Invitrogen, Carlsbad, CA) according to the manufacturer's instructions.

DRG neuronal culture and AAV5 transduction. Adult male rats were put to death with isoflurane. DRGs were collected in cold DH10 (90% DMEM/F-12 (Gibco, Grand Island, NY), 10% FBS (JR Scientific, Woodland, CA), 1% penicillin-streptomycin (Quality Biological, Gaithersburg, MD)) and then treated with enzyme solution (3.5 mg/ml dispase, 1.6 mg/ml collagenase type I in HBSS without Ca^{2+} and Mg^{2+} (Gibco)) at 37 °C. After the centrifugation, dissociated cells were resuspended in DH10 and plated at a density of 1.5×10^5 to 4×10^5 cells on glass coverslips or in a six-well plate coated with poly-L-lysine (0.5 mg/ml, Sigma, St. Louis, MO) and laminin (10 μg/ml, Invitrogen). The cells were incubated in 5% CO_2 at 37 °C. One day later, 1 μl of AAV5 virus (titer $\geq 1 \times 10^{12}$/ml) was added to each well. Cells were collected 4 d later.

Reverse transcription (RT)-PCR, rapid amplification of cDNA ends (RACE) and quantitative RT-PCR. Total RNA was extracted by the Trizol method (Invitrogen) and treated with excess DNase I (New England Biolabs, Ipswich, MA). Highly purified, DNase-treated RNA samples from human DRG were purchased from Clontech Laboratories, Inc. (Mountain View, CA). Using the Omniscript RT kit (QIAGEN, Valencia, CA) with strand-specific primers, we reverse transcribed single-stranded cDNA from RNA (1 μg). RT and PCR primers were determined from the UCSC genome database (**Supplementary Table 2**). Template (1 μl) was amplified by PCR with TaKaRa Taq DNA polymerase (Clontech Laboratories, Inc.) in 20 μl total reaction volume containing 0.5 μM of PCR primer. PCR amplification consisted of 30 s at 94 °C, 20 s at 56 °C, and 20 s at 72 °C for 35 cycles.

RNA fragments amplified from the rat DRG were extended first by using RT-PCR with strand-specific primers and then by using a RACE kit (2nd Generation, Roche Diagnostics, Indianapolis, IN). The 5′ RACE was used for amplification of the 5′-end of cDNA according to the manufacturer's instructions. The 3′ RACE analysis was performed by ligating an adaptor to the 3-hydroxyl group of the RNA, followed by gene- and adaptor-specific amplification. All primers are listed in **Supplementary Table 2**. PCR products from RT-PCR, 5′ RACE and 3′ RACE were extracted, purified and verified by automated DNA sequencing. All sequences were analyzed and the full-length Kcna2 antisense RNA sequence determined.

For quantitative real-time RT-PCR, three DRGs from three individual rats were pooled to provide enough RNA. cDNA was prepared as described above. Template (1 μl) was amplified by real-time PCR by using 1 μM of each probe and 0.5 μM of each primer listed in **Supplementary Table 2**. Each sample was run in quadruplicate in a 20-μl reaction with the TaqMan Universal PCR master mix kit (Applied Biosystems, Grand Island, NY). Reactions were performed in 96-well plates in an ABI 7500 Fast real-time PCR system (Applied Biosystems). Ratios of ipsilateral mRNA to contralateral mRNA were calculated by using the ΔCt method ($2^{-\Delta\Delta Ct}$) at a threshold of 0.02, as our pilot data indicated that the amplification reactions of the target genes and reference genes have similar PCR efficiency (**Supplementary Fig. 8a**). All data were normalized to *Gapdh*, which was demonstrated to be stable after SNL (**Supplementary Fig. 8b–d**).

For single-cell quantitative RT-PCR, freshly dissociated rat DRG neurons were first prepared as described below. Four hours after plating, small, medium and large DRG neurons were randomly collected under an inverted microscope fit with a micromanipulator and microinjector. A single living neuron was selected with a glass micropipette, without contamination by other neurons, and placed in a PCR tube with 6 μl of cell lysis buffer (Signosis, Sunnyvale, CA) as described[44]. After centrifugation, the supernatants were collected. The remaining real-time RT-PCR procedure was carried out as described[44] or according to the manufacturer's instructions with the single-cell real-time RT-PCR assay kit (Signosis).

rAAV5 plasmid constructs and virus production. After RNA was extracted from the DRG, full-length Kcna2 antisense cDNA, full-length *Mzf1* cDNA and Kcna2 sense cDNA fragment (−311 to +40) were amplified by nested RT-PCR (primers in **Supplementary Table 2**). Restriction enzyme recognition sites were introduced at the 5′ and 3′ ends of the three fragments. The PCR products were cloned by using the pGEM-T easy cloning kit (Invitrogen). The positive clones were identified by restriction enzyme analysis (BspEI/NotI) and clone sequencing.

The identified fragments were ligated into the BspEI/NotI sites of the proviral plasmids (University of North Carolina, Chapel Hill) to replace enhanced GFP (EGFP) and the S-D sequence. The resulting four vectors expressed EGFP, Kcna2 antisense RNA, Kcna2 sense fragment and MZF1 under the control of the cytomegalovirus promoter. rAAV5 viral particles carrying the four cDNAs were produced at the University of North Carolina Vector Core.

Northern blotting. To prepare complementary RNA (cRNA) probes of rat Kcna2 antisense RNA, we constructed the pSC-A plasmid, which contained a 0.946-kb DNA template, and identified the sequence using double-strand DNA sequencing. The plasmid construct was linearized by Acc65I and XhoI. A riboprobe was generated from *in vitro* transcription and labeled with ^{32}P-dUTP.

Northern blot analysis was performed as described previously[45]. The extracted RNA (10 μg) was separated on a 1.5% agarose/formaldehyde gel, transferred to a BrightStar-plus positively charged nylon membrane and cross-linked by using ultraviolet light. After prehybridization, the membrane was hybridized overnight at 68 °C with ^{32}P-dUTP-labeled cRNA probes for Kcna2 antisense RNA. After the membrane was washed and dried, autoradiography was carried out.

***In situ* hybridization histochemistry.** *In situ* hybridization histochemistry was carried out as described previously with minor modification[46,47]. Two sets of 20-μm sections were collected from each DRG by grouping every third section. *Kcna2* cRNA probe (0.268-kb fragment) and *GFP* cRNA probe (0.187-kb fragment) were prepared by *in vitro* transcription and labeled with digoxigenin-dUTP according to the manufacturer's instructions (Roche Diagnostics, Indianapolis, IN). After treatment with proteinase K and prehybridization, the two sets of sections were hybridized with digoxigenin-dUTP-labeled cRNA probes for Kcna2 antisense RNA and *GFP* RNA for 18 h at 68 °C. After being washed, the sections were incubated with alkaline phosphatase–conjugated anti-digoxigenin. The signals were developed with 5-bromo-4-chloro-3′-indolyl phosphate *p*-toluidine salt and nitro-blue tetrazolium chloride substrates. For the double labeling of *in situ* hybridization histochemistry and immunohistochemistry, the sections were treated as described above except that they were hybridized only with

doi:10.1038/nn.3438

digoxigenin-dUTP–labeled cRNA probe for Kcna2 antisense RNA and the fluorescent signals were developed with Fast Red.

Immunohistochemistry. After being blocked for 1 h at 37 °C in PBS containing 10% goat serum and 0.3% Triton X-100, the sections were incubated with rabbit anti-NF200 (1:500, Sigma-Aldrich, St. Louis, MO)[48], rabbit anti-P2X3 (1:500, Neuromics, Edina, MN)[48], biotinylated IB4 (1:100, Sigma)[48], rabbit anti-CGRP (1:500, EMD, Billerica, MA)[48], mouse anti-NeuN (1:600, EMD)[48], mouse anti-GFAP (1:500, Sigma)[48] or mouse anti-OX-42 (1:400, Sigma)[48] overnight at 4 °C. The sections were then incubated with goat anti–rabbit IgG conjugated to Cy2 (1:400, Jackson ImmunoResearch, West Grove, PA) or Cy3 (1:400, Jackson ImmunoResearch) or with FITC-labeled avidin D (1:200, Sigma) for 2 h at room temperature (25 °C). Control experiments included substitution of normal mouse serum for the primary antiserum and omission of the primary antiserum. All immunofluorescence-labeled images were examined under a Nikon TE2000E fluorescence microscope (Nikon Co., Japan) and captured with a CCD spot camera. Single- and double-labeled neurons were counted by using stereological methods as described[49].

Western blotting. For DRG, three DRGs from three individual rats were pooled to provide enough protein. The tissues were homogenized and the cultured cells ultrasonicated in chilled lysis buffer (50 mM Tris, 1 mM phenylmethylsulfonyl fluoride, 1 mM EDTA, 1 μM leupeptin). After centrifugation at 4 °C for 15 min at 1,000*g*, the supernatant was collected for cytosolic and membrane proteins and the pellet for nuclear proteins. After protein concentration was measured, the samples were heated at 99 °C for 5 min and loaded onto a 4% stacking/7.5% separating SDS-polyacrylamide gel (Bio-Rad Laboratories, Hercules, CA). The proteins were then electrophoretically transferred onto a polyvinylidene difluoride membrane (Immobilon-P, Millipore, Billerica, MA). According to the targeted protein molecular weights, the membranes were cut into several small strips and then blocked with 3% nonfat milk in Tris-buffered saline containing 0.1% Tween-20 for 1 h. The following primary antibodies were used: mouse anti-Kcna1 (Kv1.1, 1:200, NeuroMab, Davis, CA)[9], mouse anti-Kcna2 (Kv1.2, 1:200, NeuroMab)[9], mouse anti-Kcna4 (Kv1.4, 1:300, NeuroMab)[9], rabbit anti-mTOR (1:1,000, Cell Signaling Technology, Danvers, MA)[48], rabbit anti-PKCα (1:500, Santa Cruz Biotechnology, Santa Cruz, CA)[40], mouse anti-Scn10a (Nav1.8, 1:1,000; NeuroMab)[50], rabbit anti-MZF1 (1:200, provided by D.Y.H. Tuan, Medical College of Georgia)[21], mouse anti–β-actin (1:2,000; Santa-Cruz Biotechnology) and rabbit anti–histone H3 (1:1,000, Cell Signaling Technology). The proteins were detected by horseradish peroxidase–conjugated anti-mouse or anti-rabbit secondary antibody (1:3,000 Jackson ImmunoResearch) and visualized by chemiluminescence regents (ECL; Amersham Pharmacia Biotech, Piscataway, NJ) and exposure to film. The intensity of blots was quantified with densitometry.

Electrophoretic mobility shift assay. ^{32}P-labeled double-stranded DNA probe was prepared by annealing synthetic oligonucleotide in H-Star polymerase PCR solution containing ^{32}P-dCTP, dATP and dTTP at 56 °C for 1 min and then at 72 °C for 30 min. Unlabeled probe and unlabeled mutant probe were similarly prepared for use as competitors. Their oligonucleotide sequences are shown in **Supplementary Table 2**. All probes were purified in a G50 column (GE Healthcare, Silver Spring, MD). DRG nuclear extract (5 μg) was incubated with labeled probe (9 ng) alone or with 50× unlabeled probe or 50× unlabeled mutant probe at 25 °C for 20 min. Labeled probe alone was used as a control. After incubation, the DNA-protein complexes were subjected to PAGE. Autoradiography was carried out after the gel was dried. For supershift electrophoretic mobility shift assay, the nuclear extracts were incubated with rabbit MZF1 antibody (2 μg) at 25 °C for 30 min before the assay.

Chromatin immunoprecipitation assay. The homogenization solution from the DRG was cross-linked with 1% formaldehyde at 37 °C for 5 min and the reaction terminated by the addition of 0.25 M glycine. After centrifugation, the pellet was collected, washed and suspended in lysis buffer containing 0.1% SDS, 1% sodium deoxycholate and 1% NP-40 in the presence of protease inhibitors. The suspension was sonicated with an ultrasonic cell disruptor (Misonix Inc., Farmingdale, NY) to shear chromatin and produce 0.2- to 1-kb DNA fragments. After the samples were precleared with protein G–agarose, they were immunoprecipitated with 5 μg of rabbit anti-MZF1 (ref. 21), normal rabbit serum (5 μg) or rabbit anti-MZF1 (5 μg) after preabsorption with excess MZF-1 fusion protein (10 μg). Input (10% of the sample for immunoprecipitation) was used as a positive control. The fragment (156 nt) of *Kcna2* antisense gene promoter containing the predicted MZF1 binding site was detected by PCR. All primers used are listed in **Supplementary Table 2**.

Luciferase assay. To construct the *Kcna2* gene and *Kcna2* antisense gene reporter plasmids, we amplified the 1,268-bp fragment from the *Kcna2* gene promoter region and the 633-bp fragment from the *Kcna2* antisense gene promoter (including the MZF1-binding motif) by PCR from genomic DNA. The PCR products were subcloned into the SmaI and HindIII restriction sites of the pGL3-Basic vector (Promega, Madison, WI). The sequences of recombinant clones were verified by DNA sequencing. All primer sequences are shown in **Supplementary Table 2**.

HEK-293T cells were prepared as described above. After 24 h of culture, the cells were transfected with 40 ng of the pRL-TK plasmid (a normalizing control; Promega, Madison, WI) alone or plus 1 μg of the constructed plasmids using Lipofectamine 2000 (Invitrogen). After another 48 h of culture, the transfected cells were lysed with passive lysis buffer and 40 μl supernatant was assayed for luciferase activity with the Dual-Luciferase Reporter Assay System (Promega). The relative reporter activity was obtained by normalization of the firefly activity to *Renilla* activity. Three independent transfection experiments were performed.

Whole-cell patch clamp recording. To record total potassium current in DRG neurons, we first prepared freshly dissociated rat DRG neurons as described above. Whole-cell patch clamp recording was carried out 4 to 24 h after plating. Coverslips were placed in the perfusion chamber (Warner Instruments, Hamden, CT). Only green-labeled neurons were recorded. The electrode resistances of micropipettes ranged from 2 to 4 MΩ. Cells were voltage-clamped with an Axopatch-700B amplifier (Molecular Devices, Sunnyvale, CA). The intracellular pipette solution contained (in mM) potassium gluconate 120, KCl 20, $MgCl_2$ 2, EGTA 10, HEPES 10, Mg-ATP 4 (pH 7.3 with KOH, 310 mOsm). We minimized the Na^+ and Ca^{2+} component in voltage-gated potassium current recording by using an extracellular solution composed of (in mM) choline chloride 150, KCl 5, $CdCl_2$ 1, $CaCl_2$ 2, $MgCl_2$ 1, HEPES 10, glucose 10 (pH 7.4 with Tris base, 320 mOsm). Signals were filtered at 1 kHz and digitized by using a DigiData 1322A with pClamp 9.2 software (Molecular Devices). Series resistance was compensated by 60–80%. Cell membrane capacitances were acquired by reading the value for whole-cell capacitance compensation directly from the amplifier. An online P/4 leak subtraction was performed to eliminate leak current contribution. The data were stored on computer by a DigiData 1322A interface and were analyzed by the pCLAMP 9.2 software package (Molecular Devices).

To record the action potential, we switched the recording mode into current clamp. Coverslips were placed in the chamber and perfused with extracellular solution consisting of (in mM) NaCl 140, KCl 4, $CaCl_2$ 2, $MgCl_2$ 2, HEPES 10 and glucose 5, with pH adjusted to 7.38 by NaOH. The intracellular pipette solution contained (in mM) KCl 135, Mg-ATP 3, Na_2ATP 0.5, $CaCl_2$ 1.1, EGTA 2 and glucose 5; pH was adjusted to 7.38 with KOH and osmolarity adjusted to 300 mOsm with sucrose. The resting membrane potential was taken 3 min after a stable recording was first obtained. Depolarizing currents of 100–1,400 pA (200-ms duration) were delivered in increments of 100 pA until an action potential (AP) was evoked. The injection current threshold was defined as the minimum current required to evoke the first AP. The membrane potential was held at the existing resting membrane potential during the current injection. The AP threshold was defined as the first point on the rapid rising phase of the spike at which the change in voltage exceeded 50 mV/ms. The AP amplitude was measured between the peak and the baseline. The membrane input resistance for each cell was obtained from the slope of a steady-state *I–V* plot in response to a series of hyperpolarizing currents, 200-ms duration delivered in steps of 100 pA from 200 pA to −2,000 pA. The after-hyperpolarization amplitude was measured between the maximum hyperpolarization and the final plateau voltage, and the AP overshoot was measured between the AP peak and 0 mV. The data were stored on computer by a DigiData 1322A interface and were analyzed by the pCLAMP 9.2 software package (Molecular Devices). All experiments were performed at room temperature.

DRG microinjection. DRG microinjection was carried out as described[51,52]. Briefly, a midline incision was made in the lower lumbar back region and the L5 vertebral body was exposed. After the lamina was removed and the DRG exposed, viral solution (2 µl) was injected into two sites in the L4 and L5 DRGs or into one site in the L5 DRG with a glass micropipette connected to a Hamilton syringe. The pipette was removed after 10 min. After injection, the skin incision was closed with wound clips. The injected rats showed no signs of paresis or other abnormalities. The injected DRGs, stained with hematoxylin and eosin, retained their structural integrity and contained no visible leukocytes. The immune responses from viral injection were therefore minimal.

Statistical analysis. For *in vitro* experiments, the cells were evenly suspended and then randomly distributed in each well tested. For *in vivo* experiments, the animals were distributed into various treated groups randomly. All of the results are given as means ± s.e.m. Data distribution was assumed to be normal, but this was not formally tested. The data were statistically analyzed with two-tailed, paired or unpaired Student's *t*-test and a one-way or two-way ANOVA. When ANOVA showed significant difference, pairwise comparisons between means were tested by the *post hoc* Tukey method (SigmaStat, San Jose, CA). No statistical methods were used to predetermine sample sizes, but our sample sizes are similar to those reported previously in the fields[39–41]. Significance was set at $P < 0.05$.

39. Guan, X., Zhu, X. & Tao, Y.X. Peripheral nerve injury up-regulates expression of interactor protein for cytohesin exchange factor 1 (IPCEF1) mRNA in rat dorsal root ganglion. *Naunyn Schmiedebergs Arch. Pharmacol.* **380**, 459–463 (2009).
40. Singh, O.V. *et al.* Proteome of synaptosome-associated proteins in spinal cord dorsal horn after peripheral nerve injury. *Proteomics* **9**, 1241–1253 (2009).
41. Zhang, B. *et al.* Effect of knock down of spinal cord PSD-93/chapsin-110 on persistent pain induced by complete Freund's adjuvant and peripheral nerve injury. *Pain* **106**, 187–196 (2003).
42. Bennett, G.J. & Xie, Y.K. A peripheral mononeuropathy in rat that produces disorders of pain sensation like those seen in man. *Pain* **33**, 87–107 (1988).
43. Park, J.S. *et al.* Persistent inflammation induces GluR2 internalization via NMDA receptor-triggered PKC activation in dorsal horn neurons. *J. Neurosci.* **29**, 3206–3219 (2009).
44. Esumi, S., Kaneko, R., Kawamura, Y. & Yagi, T. Split single-cell RT-PCR analysis of Purkinje cells. *Nat. Protoc.* **1**, 2143–2151 (2006).
45. Gallagher, P.E. & Diz, D.I. Analysis of RNA by northern-blot hybridization. *Methods Mol. Med.* **51**, 205–213 (2001).
46. Dong, X., Han, S., Zylka, M.J., Simon, M.I. & Anderson, D.J. A diverse family of GPCRs expressed in specific subsets of nociceptive sensory neurons. *Cell* **106**, 619–632 (2001).
47. Nehmé, B., Henry, M. & Mouginot, D. Combined fluorescent in situ hybridization and immunofluorescence: limiting factors and a substitution strategy for slide-mounted tissue sections. *J. Neurosci. Methods* **196**, 281–288 (2011).
48. Xu, J.T. *et al.* Expression and distribution of mTOR, p70S6K, 4E-BP1, and their phosphorylated counterparts in rat dorsal root ganglion and spinal cord dorsal horn. *Brain Res* **1336**, 46–57 (2010).
49. Coggeshall, R.E. & Lekan, H.A. Methods for determining numbers of cells and synapses: a case for more uniform standards of review. *J. Comp. Neurol.* **364**, 6–15 (1996).
50. Ling, L. *et al.* Protein kniase B/Akt is required for complete Freund's adjuvant-induced upregulation of Nav1.7 and Nav1.8 in primary sensory neurons. *J. Pain* **14**, 638–647 (2013).
51. Han, P.J., Shukla, S., Subramanian, P.S. & Hoffman, P.N. Cyclic AMP elevates tubulin expression without increasing intrinsic axon growth capacity. *Exp. Neurol.* **189**, 293–302 (2004).
52. Xu, Y. *et al.* Adeno-associated viral transfer of opioid receptor gene to primary sensory neurons: a strategy to increase opioid antinociception. *Proc. Natl. Acad. Sci. USA* **100**, 6204–6209 (2003).